Evaluation of the thermal conductivity of porous silicon layers by an optical pump-probe method

2001 J. Phys.: Condens. Matter 13 1141

(http://iopscience.iop.org/0953-8984/13/5/327)

INSTITUTE OF PHYSICS PUBLISHING JOURNAL OF PHYSICS: CONDENSED MATTER

J. Phys.: Condens. Matter **13** (2001) 1141–1150 www.iop.org/Journals/cm PII: S0953-8984(01)17035-9

Evaluation of the thermal conductivity of porous silicon layers by an optical pump–probe method

U Bernini[1], S Lettieri[1], P Maddalena[1,3], R Vitiello[1] and G Di Francia[2]

[1] INFM, Dipartimento di Scienze Fisiche, Università di Napoli 'Federico II', Complesso Universitario di Monte S Angelo, Via Cintia, I-80126 Napoli, Italy
[2] ENEA-CRIF 'Centro Ricerche Fotovoltaiche', Località Granatello, I-80055, Portici (Napoli), Italy

E-mail: pasmad@na.infn.it (P Maddalena)

Received 11 September 2000

Abstract

Measurements of the thermal conductivity for free-standing porous silicon layers were performed by means of an optical pump–probe experimental set-up. By transient heating due to laser pumping, a refractive index modulation was induced in the sample and, solving the heat propagation equation for inside the solid film, it is shown that the time decay of the nonlinear transmittance can be related to the thermal conductivity. The optical technique demonstrated here is contactless, quite simple and does not require much effort in data analysis, and is therefore very useful for thin-film characterization. The thermal conductivities of the porous silicon samples, whose porosities lay in the range 60–70%, were taken into account, and we found good agreement with results obtained with different techniques.

1. Introduction

In the last ten years, a major part of the scientific and technological research effort on the properties of porous silicon (PS) has been concerned especially with its possible application in optoelectronics, as it is a leading contender in the race towards silicon-based photonics. Notwithstanding this, a very large and growing interest in PS as a passive material for various kinds of technological application (such as waveguiding, micromachining and gas sensing) has been developing, as the fabrication of PS is simple and not expensive, and as present technological knowledge allows one to control its peculiar morphology quite confidently.

Among the fields of interest as regards PS, in more recent years attention has been devoted to its thermal characterization, since the use of PS as thermally insulating layers in sensing devices appears promising. In fact, one of the problems in the fabrication of differential-temperature-based sensor devices (such as thermopiles and microbolometers) is the high thermal conductivity of c-Si (156 W mK^{-1} at room temperature). When a sensing element is

[3] Author to whom any correspondence should be addressed. Telephone: +39-081-676126; fax: +39-081-676346.

integrated on silicon wafers, c-Si would lead to an unwanted heat dispersion that would reduce the sensitivity of the device. So micromachining technologies have to be used in order to obtain free-standing microstructures (such as bridges, membranes, cantilevers) separated from the rest of the device by a thin air gap and reduction of the thermal flux from hot regions to the cold rim of the sensors [1–3]. These structures have the advantage of low thermal conductance but the obvious disadvantage of mechanical vulnerability.

PS offers an alternative approach to the problem as it is a good thermal insulator, having a thermal conductivity two or three orders of magnitude lower than that of c-Si (depending on the particular sample morphology and porosity), and so it is possible to deposit the sensing elements on a PS layer, realizing both a satisfactory thermal insulation and a useful mechanical solidity.

The low thermal conductivity K of PS has been pointed out in the last few years by different authors [4–12] using different approaches. The results of some of those experimental works have been summarized in a review paper [13], in which it is evidenced that the results show a significant reduction of K with respect to the bulk value: it is to be noted that the results reported show significant scatter because of the morphology and fabrication parameter differences. Values from 31 W mK^{-1} for macroporous n-type PS [10] to about 0.05 W mK^{-1} for high-porosity p-type samples [5] have been measured. It has been shown that the thermal conductivity of PS is usually higher for macroporous PS (typical nanostructure dimensions: micrometres) than in mesoporous and nanoporous PS (from a few nanometres to a few tens of nanometres). As regards microporous silicon, consistent reduction of K has been shown in the literature [13]. These results are easy to explain, as the thermal insulating properties of PS are mainly due to two causes. First, the 'sponge'-like morphology of the material, which can be described as a more or less disordered ensemble of nanostructures (whose dimensions depend on the substrate and on the fabrication parameters), hinders thermal transport: this effect is larger when the nanocrystals are smaller and the porosity increases, as in mesoporous and microporous PS. Second, the thermal insulation is enhanced by the presence of air (whose thermal conductivity $K_{\mathrm{air}} = 0.026$ W mK^{-1} is very low) inside the pores.

Different techniques have been used in the literature to measure the thermal conductivity of PS. In references [4, 5] microdevices are used to generate and analyse directly a thermal wave on the PS layer. The most widely used technique is probably the photoacoustic method, used in references [6–11]. Recently it has been shown in reference [12] that an indirect measure of the thermal conductivity can be obtained by monitoring the Stokes shift of the backscattering Raman peak for a given laser-induced heating of the sample. Each of those techniques has both advantages and disadvantages. The use of microdevices as in reference [4] introduces contact problems and, since the temperature sensors are directly attached to the sample surfaces, they must be covered by an insulating layer, whose effect should be removed from the experimental data. In the Raman-scattering-based method the results should be accurate only for samples whose thickness is greater than the pump laser beam waist on the sample plane (in practice, one is restricted to samples of thickness $\sim$50 micrometres or more). The photoacoustic method is a well established and well known technique; it gives an indirect measure as the thermal conductivity is extrapolated from the fitting of experimental results, and usually a quite extensive numerical analysis effort is needed.

In this paper we present contactless measurements of the thermal conductivity of thin PS free-standing layers having different porosities. The experimental set-up that we used was a time-resolved optical pump and probe, where the absorption of the pulsed pump beam induces changes in the refractive index of the layer, which are manifested in a change of the transmitted fraction of the probe laser. This is a standard set-up for the investigation of optically induced nonlinearities, and can also be used for investigation of carrier recombination times in crystals.

In the present work the pump-and-probe set-up was used as a 'thermal analyser', pumping the sample with relatively long light pulses whose frequency is within the absorption band of the material. By 'long' pulses, we mean that the energy transfer to the sample is significant, so fast optical nonlinearities related to virtual transitions of bound carriers in the semiconductor (the pure electronic Kerr effect) are negligible and heating effects are dominant. In the next section the experimental set-up and the samples investigated are described, while in the third section the results will be given and discussed.

2. Theory

When an intense laser beam impinges on a solid film, nonlinear optical effects may be observed. The simplest way to observe optical nonlinearities is to use two different beams, in the pump–probe configuration described above. The observation of nonlinear transmittance of the probe beam can give information on the physical mechanisms involved in the optical nonlinearity and so a contactless characterization of the material can be performed. When a continuous-wave probe is used to investigate the transient change of the complex refractive index induced by a fast pump pulse, it is possible to determine the typical recovery time of the induced nonlinearity. When the pump wavelength lies in the absorption range of the sample, typically two kinds of nonlinear effect can arise. The first is related to the change in the number of excited carriers in the crystal (pair generation) which induces a change in refractive index and which decays within the lifetime of the excited pairs. The second, which is usually relevant, is related to the change of the local temperature due to light absorption (phonon excitation). The decay of the optical nonlinearity related to this latter effect depends on the time evolution of the heat in the sample and so involves its heat conductivity.

Typical carrier lifetimes in PS are of the order of 10–100 μs, as is shown in the literature [14], and optical nonlinearities having longer decay times, such as the ones that we show in this paper, have to be attributed to thermal effects: from the detection of such effects, the thermal conductivity of the PS layers can be determined.

Let us consider a dielectric film: its optical transmittance τ at normal incidence is related to the complex refractive index $\widetilde{n}_0 = n_0 + \mathrm{i}\kappa_0$. Thus for a small change in refractive index, the transmittance $\tau(n, \kappa)$ changes according to

$$\Delta\tau = \left(\frac{\partial\tau}{\partial n}\right)_{n_0} \Delta n + \left(\frac{\partial\tau}{\partial\kappa}\right)_{\kappa_0} \Delta\kappa$$

and when this is thermally induced:

$$\Delta n = \frac{\partial n}{\partial T}\,\Delta T$$

$$\Delta\kappa = \frac{\partial\kappa}{\partial T}\,\Delta T$$

where T is the temperature; thus, in a first-order approximation, the modulation in transmittance can be related to the temperature change by a linear law:

$$\Delta\tau = \left(\frac{\partial\tau}{\partial n}\frac{\partial n}{\partial T} + \frac{\partial\tau}{\partial\kappa}\frac{\partial\kappa}{\partial T}\right)\Delta T = F(\widetilde{n}_0)\,\Delta T.$$

The time profile of a temperature change in a solid slab induced by a laser pulse source can be obtained using the formalism of the 'instantaneous heat source', i.e. using a Green function technique [15]. This latter technique consists in using an elementary solution $F(r, r', t)$ which acts at $t = 0$ as a Green function for the differential equation; i.e.,

$$\left[\nabla_r^2 - \frac{1}{\alpha}\frac{\partial}{\partial t}\right] F(r, r', t) = 0 \tag{1}$$

where

$$F(r, r', t = 0) = \delta(r - r') \tag{2}$$

and where $\alpha = K/\rho c_p$ is the thermal diffusivity, K the thermal conductivity, ρ the density and c_p the specific heat. The physical meaning of such a function is the temperature induced by an instantaneous point source of heat, acting at $t = 0$ on the point $\boldsymbol{r}'$. It can easily be shown that such a Green function is given by

$$F(r, r', t) = \frac{Q}{\pi\alpha t} \exp\left\{\left[(x - x')^2 + (y - y')^2 + (z - z')^2\right]/4\alpha t\right\}. \tag{3}$$

The temperature induced by an instantaneous and extended point source is obtained by integrating this elementary solution over the spatial variables (x', y', z'). This approach allows to solve the heat equation in particular cases, in which a regular geometry of the heat source and the temperature distribution on the heated body at $t = 0$ are given. Notwithstanding this, most geometries lead to solutions that cannot be expressed in closed analytical form. As the case of interest here is a thin solid film which is heated by a laser pulse, the illumination and then the heating take place instantaneously along the propagation axis z of the laser, so in the heat conduction the z-coordinate is in practice irrelevant and the problem can be recast as a bidimensional one. The heat source can be approximated with a cylindrical geometry having the beam waist of the pump laser on the sample plane as the radius a. In order to obtain an analytical result for the temperature transient, some approximations have to be made. First, neglecting the field energy-density drop inside the thin film, one can approximate the initial temperature of the film induced by the instantaneous pump pulse with a step function:

$$f(r) = \begin{cases} T_0 & \text{for } r < a \\ 0 & \text{for } r > a. \end{cases} \tag{4}$$

The temperature induced by an instantaneous cylindrical source with initial temperature $f(r)$ is given by [15]

$$T = \frac{1}{2\alpha t} \int_0^\infty \exp\left[-(r^2 + r'^2)/4\alpha t\right] I_0\left(\frac{rr'}{2\alpha t}\right) f(r') r' \, \mathrm{d}r' \tag{5}$$

where I_0 is the zero-order modified Bessel function. When the initial condition, given by equation (4), is used, equation (5) becomes

$$T = \frac{T_0}{2\alpha t} \exp\left(-\frac{r^2}{4\alpha t}\right) \int_0^a \exp\left(-\frac{r'^2}{4\alpha t}\right) I_0\left(\frac{rr'}{2\alpha t}\right) r' \, \mathrm{d}r'. \tag{6}$$

This integral is called a P-function and must be evaluated numerically. A tabulation can be found in reference [16]. It can be solved analytically only on the axis $r = 0$, where it gives

$$T(r = 0, t) = T_0(1 - \exp(-a^2/4\alpha t)). \tag{7}$$

This simple decay behaviour can be used as an approximation of the effective decay of the probe signal at $t > 0$, where $t = 0$ indicates the arrival of the pump pulse. If the probe pulse spot size a_p on the input face of the sample is less than the pump beam one, the decay of the transmitted probe signal can be approximated by equation (7). Then, fitting the experimental curves with a decay time $\tau_0 = a^2/4\alpha$ as a parameter and measuring the pump spot size a, a determination of the thermal diffusivity, and hence of the thermal conductivity, can be obtained. In the following the experimental results are given.

3. Experimental set-up and results

The experimental set-up is shown in figure 1. The pump pulse is obtained from a Q-switched continuum Nd:YAG laser, whose pulse duration and wavelength are 5 ns and 1064 nm respectively. A $\lambda/2$ waveplate, coupled with a birefringent polarizer, provides a variable attenuation of the pulse intensity, and in order to avoid damaging the sample, coloured filters are used to reduce the infrared energy pulse. The pulse is then focused on the sample at pulse energies ranging between 0.1 and 5.0 mJ.

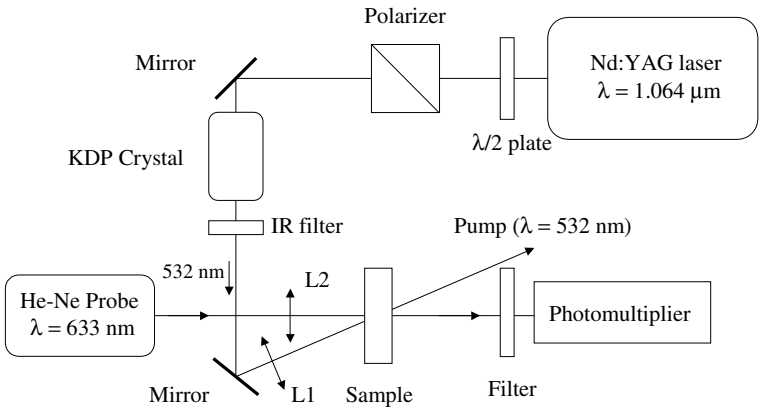

Figure 1. The experimental pump-and-probe set-up.

The probe beam is provided by a Melles-Griot He–Ne 3 mW power laser. The probe beam is also equipped with a variable-attenuation system given by two adjustable dichroic polarizers. To detect the probe light, a side-on photomultiplier (PM) was chosen in order to maximize the detection area and the sensitivity. Care was taken to not exceed the average anodic current of the detector, since, when this limit is exceeded, the long-term reproducibility of the signal from the photomultiplier anode can be damaged and the detected signal is somewhat distorted and saturated. The laser beams were not collinear, as shown in figure 1; this was in order to minimize detection of unwanted signals by the PM and in order also to allow independent focusing of the pump and probe beams (using lenses with different focal lengths) and so to produce a probe beam waist on the sample slightly smaller than the pump beam waist. However, on increasing the angle between the pump and probe beams, the overlapping of the beams inside the sample, and thus the detected modulation signal, are reduced: so an 'almost collinear' beam configuration was chosen. A proper choice of the coupling resistor at the input channel of the scope provided a high sensitivity to any modulating signal. This configuration, however, has the disadvantage of being very sensitive to noise, and so the curves that we report were obtained by averaging over 500 acquired signals, while the laser repetition rate was fixed at 1 Hz to avoid possible cumulative heating effects due to long light exposure of the sample.

In order to test the accuracy of the results obtained with this experimental set-up, a preliminary measurement was made on a material of known thermal conductivity. We used a KG3 Schott coloured filter, which is transparent in the visible range and is highly absorptive in the near infrared. The filter was pumped by the Nd:YAG Q-switched laser ($\lambda = 1064$ nm) and the pump laser pulses were focused by a converging lens of focal length $f = 40$ cm. The beam waist of the laser pump at the sample position was measured with a scanning knife-edge technique, giving $a = 104 \pm 4$ μm. The time-resolved transmittance is shown in figure 2, where the dots represent the experimental data and the continuous line is the best-fit curve

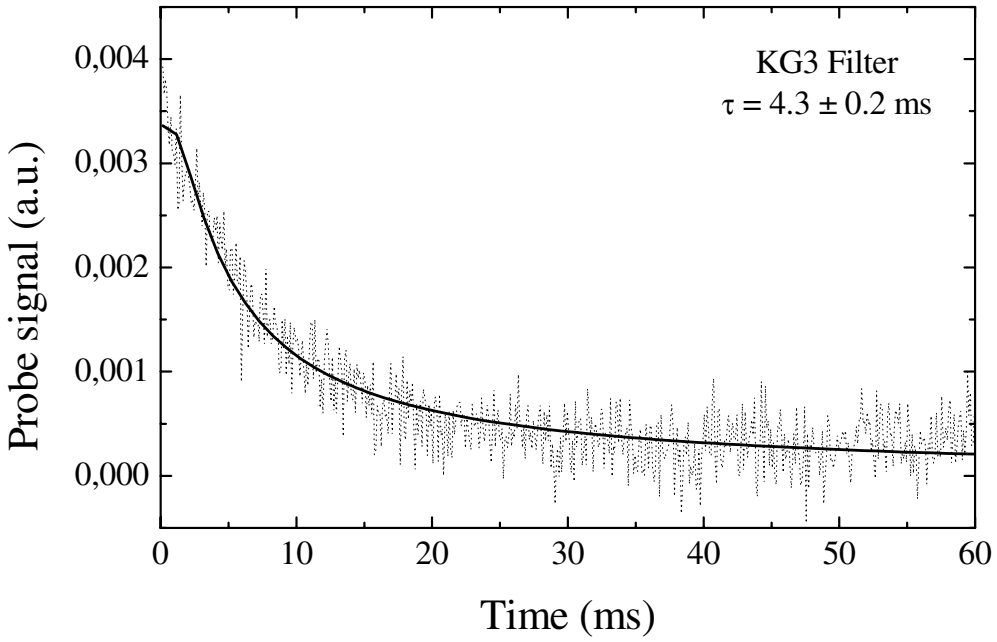

Figure 2. Nonlinear probe transmittance through the KG3 filter pumped with a Nd:YAG beam at $\lambda = 1064$ nm. The dots are the experimental points, while the solid line is the best-fit curve based on equation (7).

obtained using equation (7). From the extracted time constant, and taking from the literature the values of the density and specific heat of the glass ($\rho = 2.5\ \mathrm{g\,cm^{-3}}$, $C_p = 0.75\ \mathrm{J\,g^{-1}\,K^{-1}}$), the measured thermal conductivity is $K = 1.18 \pm 0.11\ \mathrm{W\,m^{-1}\,K^{-1}}$, which is very consistent with the value found in the literature ($K = 1.1\ \mathrm{W\,m^{-1}\,K^{-1}}$) [17].

Next we considered porous silicon layers. Free-standing PS can be easily obtained by the standard lift-off procedure, and samples which are highly transmitting in the visible range can be easily obtained. As the absorption of porous silicon is usually negligible in the near infrared, the pump wavelength was changed, using a frequency-doubling KDP crystal in order to obtain green-light pump pulses ($\lambda = 532$ nm).

Samples having high transmittance in the red region and high absorbance in the green region were fabricated by means of the etching parameters shown in table 1, where also the porosities and the thicknesses of the three prepared samples (S1, S2, S3) are shown. Both the porosity, measured by a gravimetric method, and the thickness, measured by a mechanical profilometer, were determined for samples prepared under the same experimental conditions, i.e. with the same etching parameters, as the ones investigated, due to the destructive nature of these measurements. Of course, this can be done thanks to the high repeatability of the fabrication method. Preliminary measurements of the transmission of the samples were performed with a Perkin-Elmer NIR-VIS spectrometer; the results are shown in figure 3. The samples were stored for about two months in air before the measurements, so it is reasonable to assume that oxidation developed inside the samples. In any case, oxidation should not have an important influence on the thermal conductivity of high-porosity PS samples [12, 13].

As has been said, the pump beam was provided by the second harmonic of the Nd:YAG laser, at $\lambda = 532$ nm. The pump beam was focused on the PS samples by means of a converging lens of 30 cm focal length, and the measurement of the laser spot size on the sample, performed

Table 1. Fabrication parameters, porosities and thicknesses of the samples.

Sample	S1	S2	S3
Doping type	p	p	p
Resistivity (Ω cm)	0.7–1.3	0.7–1.3	0.7–1.3
HF concentration (%)	70 + IPA	70 + IPA	70 + IPA
Etching duration (min)	30	20	40
Current density (mA cm^{-2})	13.2	26.4	26.4
Porosity (%)	61	66	73
Thickness (μm)	19	27	38

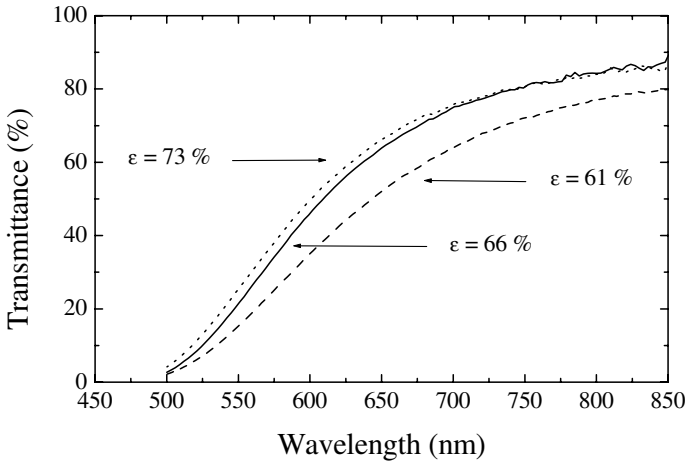

Figure 3. Transmittance curves for the porous silicon samples S1, S2 and S3.

with the knife-edge technique, gave $a = 82 \pm 2$ μm. In figures 4, 5 and 6, the time-resolved probe signals are shown, together with the best-fit curves. For the PS specific heat the bulk silicon value $C_p = 0.713$ J g^{-1} K^{-1} was used as in reference [10], and the porous silicon density can be simply obtained when the porosity of the sample and the bulk silicon density $\rho_{c-Si} = 2.32$ g cm^{-3} are given. The results are summarized in table 2. We can see that no clear evidence of correlation between the thermal conductivity and porosity is obtained. This is a consequence of the fact that the average macroscopic porosity does not give direct information on the material morphology at a microscopic scale; more precisely, what mainly influences the heat flow into the medium is the transverse dimensions of the porous silicon skeleton and this is not completely taken into account by the porosity parameter, which is a macroscopic average over the sample morphology. Probably, even if the average dimensions of the nanoparticles

Table 2. Measured thermal conductivities.

Sample	Thermal conductivity (W mK^{-1})
S1	$(1.5 \pm 0.1) \times 10^{-1}$
S2	$(1.3 \pm 0.1) \times 10^{-1}$
S3	$(1.70 \pm 0.14) \times 10^{-1}$

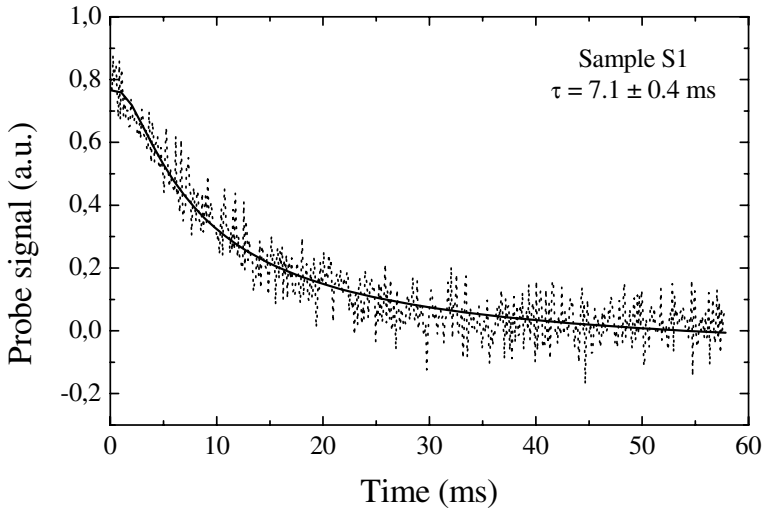

Figure 4. Nonlinear probe transmittance through sample S1 pumped with the second harmonic of a Nd:YAG beam at $\lambda = 532$ nm. The dots are the experimental points, while the solid line is the best-fit curve based on equation (7).

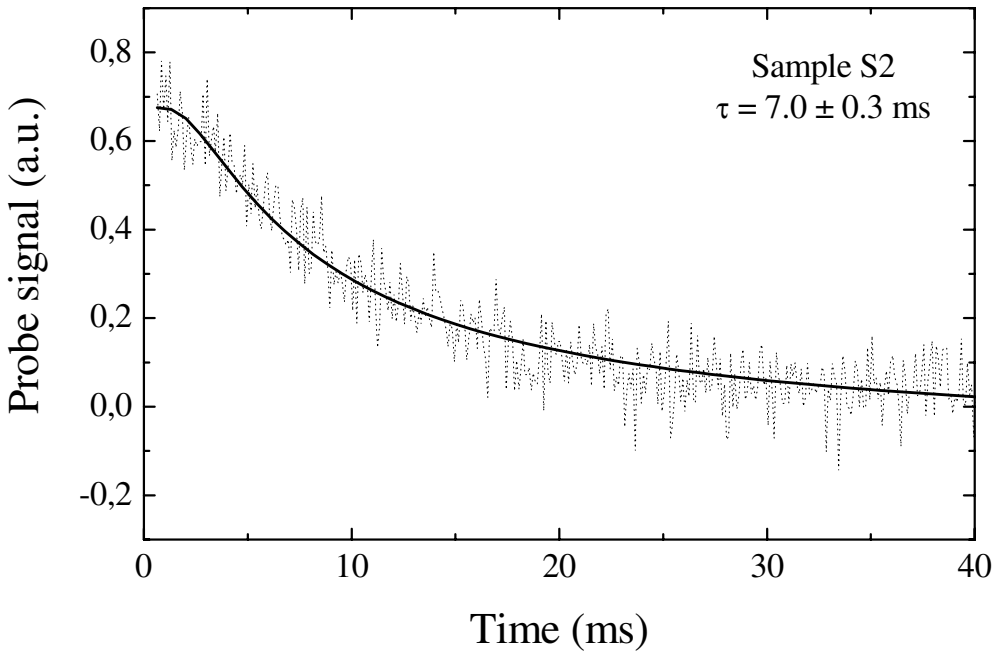

Figure 5. Nonlinear probe transmittance through sample S2 pumped with the second harmonic of a Nd:YAG beam at $\lambda = 532$ nm. The dots are the experimental points, while the solid line is the best-fit curve based on equation (7).

constituting the samples may be different, they are all of the order of magnitude of a few nanometres, and this fact is evident in the significant reduction of the thermal conductivity (with respect to crystalline silicon) which is observed for each sample. The small differences

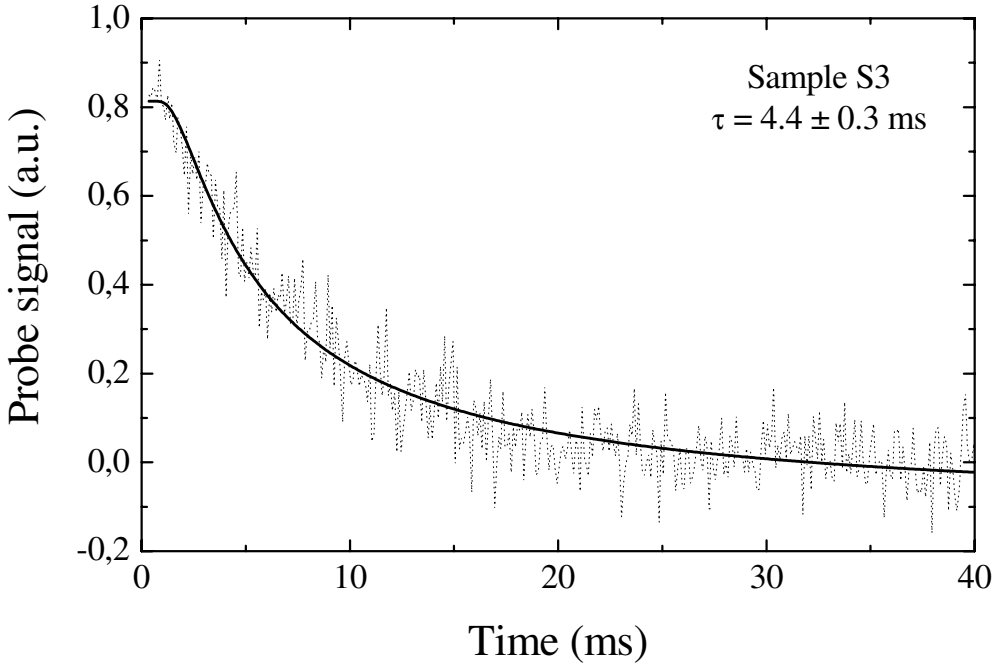

Figure 6. Nonlinear probe transmittance through sample S3 pumped with the second harmonic of a Nd:YAG beam at $\lambda = 532$ nm. The dots are the experimental points, while the solid line is the best-fit curve based on equation (7).

between the measured thermal conductivities of the samples investigated can be explained as a consequence of different specific surfaces and size distributions.

A possible source of systematic errors in our measurements was that it was not possible to fully satisfy the condition of the probe beam waist being much smaller than the pump beam waist on the sample (as it was $a_p \simeq 60$ μm). Notwithstanding this, our results are in quite good agreement with those reported in references [6] and [5]. In reference [6] the value of $K = 0.15$ W mK^{-1} is reported for a p+ sample, while in [5] values of $K = 0.14$ W mK^{-1} and $K = 0.18$ W mK^{-1} are reported for the room temperature thermal conductivity for p-type PS layers having porosities of $\varepsilon = 64\%$ and $\varepsilon = 74\%$ respectively.

4. Conclusions

Measurements of thermal conductivities of porous silicon layers of different porosities are given. In order to avoid some of the disadvantages usually related to the most often used techniques, we proposed a new method which is based on an optical pump and probe. The method has the advantage of being contactless and simple, permitting reduced data analysis; it also permits one, at the same time, to investigate the electronic recombination times with the same experimental set-up just by changing the laser beam parameters. The effectiveness of the method was tested on a coloured glass sample of known thermal conductivity, and very good agreement with the expected result was obtained. The values that we report for the thermal conductivity are in agreement with those given in other reports that were obtained using different techniques, confirming the fact that high-porosity nanoporous silicon has thermal conductivities three orders of magnitude lower than the bulk one.

References

[1] Werno J, Kersjes R and Vogt H 1994 *Sensors Actuators* **42** 578
[2] Zhang X and Grigoropoulos C P 1995 *Sci. Instrum.* **66** 1115
[3] Lang W 1997 *Structural and Optical Properties of Porous Silicon Nanostructures* ed G Amato, C Delerue and H J von Bardeleben (New York: Gordon and Breach)
[4] Drost A, Steiner P, Moser H and Lang W 1995 *Sensors Mater.* **7** 111
Lang W, Drost A, Steiner P and Sandmaier H 1995 *Mater. Res. Soc. Symp. Proc.* **358** 561
[5] Gesele G, Linsmeier J, Drach V, Fricke J and Arens-Fischer R 1997 *J. Phys. D: Appl. Phys.* **30** 2911
[6] Theiss W *et al* 1995 *Proc. SPIE* **2089** 176
[7] Obraztsov A N, Timoshenko V Yu, Okushi H and Watanabe H 1997 *Semiconductors* **31** 534
[8] Benedetto G, Boarino L and Spagnolo R 1997 *Appl. Phys.* A **64** 155
[9] Blonskij I V, Brodyn M S, Tkhoryk V A, Filin A G and Piryatiaskij J P 1997 *Semicond. Sci. Technol.* **12** 11
[10] Benedetto G, Boarino L, Brunetto N, Rossi A, Spagnolo R and Amato G 1997 *Phil. Mag.* B **76** 383
[11] Bernini U, Maddalena P, Massera E and Ramaglia A 1999 *Opt. Commun.* **168** 305
[12] Perichon S, Lysenko V, Remaki B and Barbier D 1999 *J. Appl. Phys.* **86** 4700
Lysenko V, Perichon S, Remaki B and Barbier D 1999 *J. Appl. Phys.* **86** 6841
[13] Lang W 1997 *Properties of Porous Silicon (EMIS Datareview Series No 18)* ed L Canham (London: Inspec) p 138
[14] Cullis A G, Canham L T and Calcott P D J 1997 *J. Appl. Phys.* **82** 909
[15] Carslaw H S and Jaeger J C 1959 *Conduction of Heat in Solids* 2nd edn (Oxford: Clarendon) ch 10
[16] Masters L 1955 *J. Chem. Phys.* **23** 1865
[17] Kaye G W C and Laby T H 1973 *Tables of Physical and Chemical Constants* (London: Longman) p 60